Toward practical application of functional conductive polymer binder for a high-energy lithium-ion battery design

Hui Zhao,[a] † Zhihui Wang,[a] † Peng Lu,[b] Meng Jiang,[b] Feifei Shi,[c] Xiangyun Song,[a] Ziyan Zheng,[a,d] Xin Zhou,[a,e] Yanbao Fu,[a] Guerfi Abdelbast,[f] Xingcheng Xiao,[b] Zhi Liu,[g] Vincent S. Battaglia,[a] Karim Zaghib,[f] and Gao Liu[a*]

[a]*Environmental Energy Technologies Division and* [c]*Materials Sciences Division, Lawrence Berkeley National Laboratory, Berkeley, California, 94720, United States*

[b]*Global Research & Development Center, General Motors, Warren, Michigan, 48090, United States*

[d]*University of California, Berkeley, California, 94720, United States*

[e]*University of California, Los Angeles, California, 90095, United States*

[f]*Institut de recherche en électricité d'Hydro-Québec (IREQ), Montreal, Canada*

[g]*State Key Laboratory of Functional Materials for Informatics, Shanghai Institute of Microsystem and Information Technology, Chinese Academy of Sciences, Shanghai 200050, China.*

[*] Tel.: +1-510-486-7207; fax: +1-510-486-7303; Email: gliu@lbl.gov (G. Liu)

† These authors contributed equally to this work

Abstract: Silicon alloys have the highest specific capacity when used as anode material for lithium-ion batteries, however, the drastic volume change inherent in their use causes formidable challenges toward achieving stable cycling performance. Large quantities of binders and conductive additives are typically necessary to maintain good cell performance. In this report, an only 2% (by weight) functional conductive polymer binder without any conductive additives was successfully used with a micron-size silicon monoxide (SiO) anode material, demonstrating stable and high gravimetric capacity (> 1000 mAh/g) for ~500 cycles and more than 90% capacity retention. Prelithiation of this anode using stabilized lithium metal powder (SLMP®) improves the first cycle Coulombic efficiency of a SiO/NMC full cell from ~48% to ~90%. The combination

enables good capacity retention of more than 80% after 100 cycles at C/3 in a lithium-ion full cell.

Keywords: silicon monoxide, conductive polymer binder, stabilized lithium metal powder (SLMP), lithium ion battery

Considerable efforts have been devoted to increasing the energy densities of lithium-ion batteries, in order to fulfill the demand for application in consumer electronics and electric vehicles (EVs)/plug-in hybrid vehicles (PHEVs). To further increase the energy density of the lithium-ion battery, new materials are being developed for higher capacity or increased cell voltage. All these materials choices pose new challenges when integrated into the lithium-ion electrode and into practical cell geometry. State-of-the-art lithium-ion technology uses graphite as an anode, with a theoretical gravimetric specific capacity of 372 mAh/g, while the alternative alloy anode materials such as tin (Sn, 994 mAh/g) or silicon (Si, 4200 mAh/g) have much higher gravimetric specific capacities.[1] However, almost 300% volume expansion occurs as the material transitions from Si to its fully lithiated phase.[2] Because of this large volume change, the electronic integrity of the composite electrode is disrupted, and high and continuous surface side reactions are induced, leading to a drastic capacity decay.[3] Associated with these problems is that most of the current approaches in Si materials research have only achieved an areal capacity less than 1 mAh/cm^2 [4] unless electrode architecture designs are integrated into the electrode fabrication process.[5,6]

Silicon monoxide (SiO) has been considered a promising alternative anode material for lithium-ion batteries (LIBs). The study of the microstructure of SiO and its transformation during lithiation and delithiation have been on-going topics.[7] A random mixture model is normally used to describe the microstructure of SiO, which indicates that SiO has two separate phases in nanodomain, Si (Si^0) and SiO_2 (Si^{4+}).[8, 9] The SiO_2 inactive phase could buffer the volume change during lithiation and delithiation of the Si phase, as well as alleviate the stress during cycling and restrain the pulverization of the active Si phase. Most of the SiO-based materials have capacities at

1000~2000 mAh/g. The higher specific capacity leads to faster capacity decay. With a specific capacity of ~1000 mAh/g, the volume change is limited to ~50% on the particle level. The high specific capacity (three times that of carbon) and relatively low volume expansion, combined with a small initial specific surface area, make the SiO materials an attractive alternative to pure Si or Sn materials. However, the usage of SiO as an additive in a graphite electrode has been limited into a few percent due to the lack of an effective method to assemble high concentration of SiO materials. Strong adhesion is required to withhold the electrode structure of SiO during charge and discharge, as is uniform electronic conduction at the particle interface level and electrode level. Although a higher concentration of binder and conductive additive can fulfill these requirements, these inactive species (binder and carbon black) decrease the electrode level energy density to the extent that makes it less competitive than the state-of-the-art graphite electrode.

In this work, we demonstrate a SiO electrode with a high concentration (98%) of active SiO and only 2% of binder without any conductive additives. This SiO electrode can be reversibly cycled for 500 times with more than 90% capacity retention. The SiO electrode has a reversible capacity three times higher than that of the graphite electrode. The prelithiation of this anode using stabilized lithium metal powder (SLMP®) improves the first-cycle coulombic efficiency of a SiO/NMC full cell from ~48% to ~90%. A practical lithium ion cell shows good capacity retention of more than 80% after 100 cycles at a C/3 rate.

Results

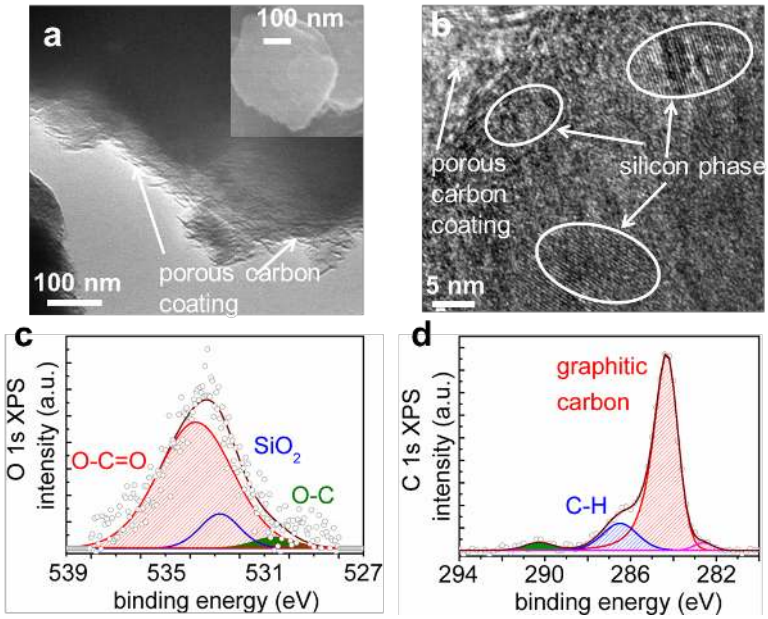

Figure 1. (a) TEM image of the carbon-coated SiO particle, indicating the porous nature of the carbon coating. The inset shows the SEM image of a single SiO particle, both with a scale bar of 100 nm. (b) HRTEM image of the SiO particle. The white circles indicate the Si nano-domains within the SiO_2 matrix. The amorphous carbon coating is at the outer surface of the SiO particles. (c) and (d) The observation of SiO_2 and carbon coating from XPS spectra was acquired simultaneously at the outer surface of the SiO materials, with a depth penetration of 2~4 nm. Open circles are experimental data, while solid lines are the results of a Gaussian deconvolution fitting.

The SiO material and functional conductive polymer binder. The SiO materials are made into micron-size particles with specific surface area of 1~10 m^2/g, depending on the particle sizes, as opposed to the surface area of typical nano-Si materials at 20~100 m^2/g.[10] Unlike Si material that exposes the reactive Li_xSi phase to the electrolytes during the lithiation process, most of the reactive Si phases are enclosed in the SiO_2 matrix (Figure 1a, b, d). The side reactions between electrolytes and Li_xSi during charge and discharge are significantly reduced. However, the introduction of the SiO_2 phase and the micron size of the particle significantly reduce the electronic conduction of the particles.[11] A carbon coating (~ 10 wt%, by elemental analysis) on the surface of SiO particle is used to increase the electronic conductivity (Figure 1a, b, d).[12] This carbon coating can be controlled to be a porous structure with a partially exposed SiO surface (Figure 1a) to facilitate ion transport. The BET method shows that the surface area of the particle

is 11.92 m^2/g, with a calculated particle diameter of 234 nm. A bimodal size distribution of SiO particles is shown by both particle size analysis (PSA, Figure S1a) and SEM (Figure S1b), with small particles of 1~2 μm and big particles of >10 μm. The larger surface area measured by BET also indicates the porous nature of the carbon coating on the SiO particle surface, which is further corroborated by the XPS data (O 1s and C 1s) of the pristine carbon-coated SiO particles in Figure 1 c and d. Both the carbon coating and the SiO_2 are clearly detected on the particle surface.[13]

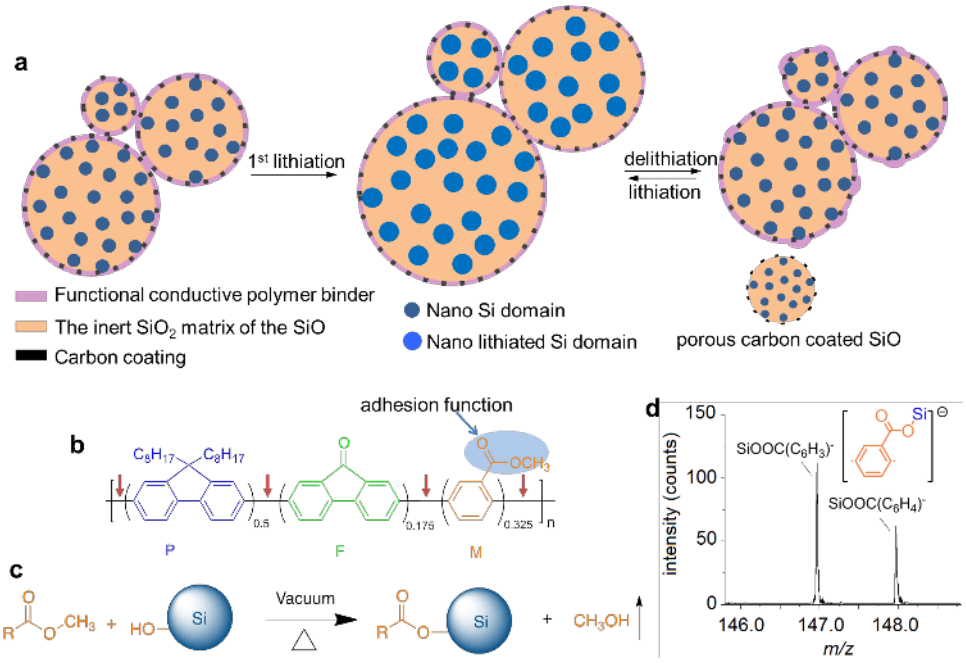

Figure 2. (a) The schematic of an electrode design with low concentration of functional conductive polymer binder and SiO, enabled by strong adhesion of covalent functionality and electronic conduction of functional conductive polymer binder. (b) The chemical structure of the PFM functional conductive polymer binder. The red arrows indicate the most likely chemical bonds to be broken during the ionization process in the TOF-SIMS measurement. The blue shadow highlights the ester group that forms adhesion bonds with the SiOH surface. (c) The trans-esterification reaction between the ester functional group of the PFM binder and the SiOH surface group, which provides strong adhesion, during the electrode drying process. (d) The TOF-SIMS result of the binder and active materials interface that shows the evidence of chemical bonding between the binder and the active materials.

Although SiO has demonstrated good cyclability and low surface reaction,[14] two major obstacles limit this material of reaching its full potential in LIBs: the excessive volume change of the micron-size particles, and the consumption of Li (low first-cycle coulombic efficiency) during the activation process. The large volume change causes the failure between the adhesive binder

and the SiO materials.[15] More conductive additives and binder have to be used to fabricate an electrode with an acceptable conductivity and mechanical strength to withstand the volume change.[16,17] The use of excessive inactive materials significantly reduces the electrode level capacity close to the graphite-based electrode. However, a functional conductive polymer binder, Poly (9,9-dioctylfluorene-co-fluorenone-co-methylbenzoic ester) (PFM, Figure 2b), was developed by combining adhesion and electrical conduction to provide molecular-level electronic connections between the active material and the conductive polymer matrix.[18,19,20] The polar ester functional group, which is designed for the adhesion with the SiO_2 surface, is especially suitable for the SiO material. Methylbenzoic ester groups on PFM form chemical bonding with the hydroxide-terminated SiO_2 surface via a trans-esterification reaction (Figure 2c). The formation of this strong chemical bond between the SiO and PFM can be observed in the TOF-SIMS results, shown in Figure 2d.[21] The detection of high contents of the $SiOO(C_6H_3)^-$ species at the interface of the binder and Si confirms that the SiO active material particles are bonded with PFM, which could be further corroborated by the TOF-SIMS data shown in Figure S2. Since the SiO_2 domains remain dimensionally stable in subsequent charge and discharge reactions after the first-cycle lithiation, and they are part of the stable surface of the SiO materials, the adhesion between PFM and SiO materials is much more effective than with Si in the previous report.[18] Moreover, the use of the conductive PFM binder eliminates the use of a conductive additive. The improved adhesion between PFM and SiO, combined with the conductive nature of PFM, considerably increases the loading of active material and improves the energy density of the lithium-ion cell.

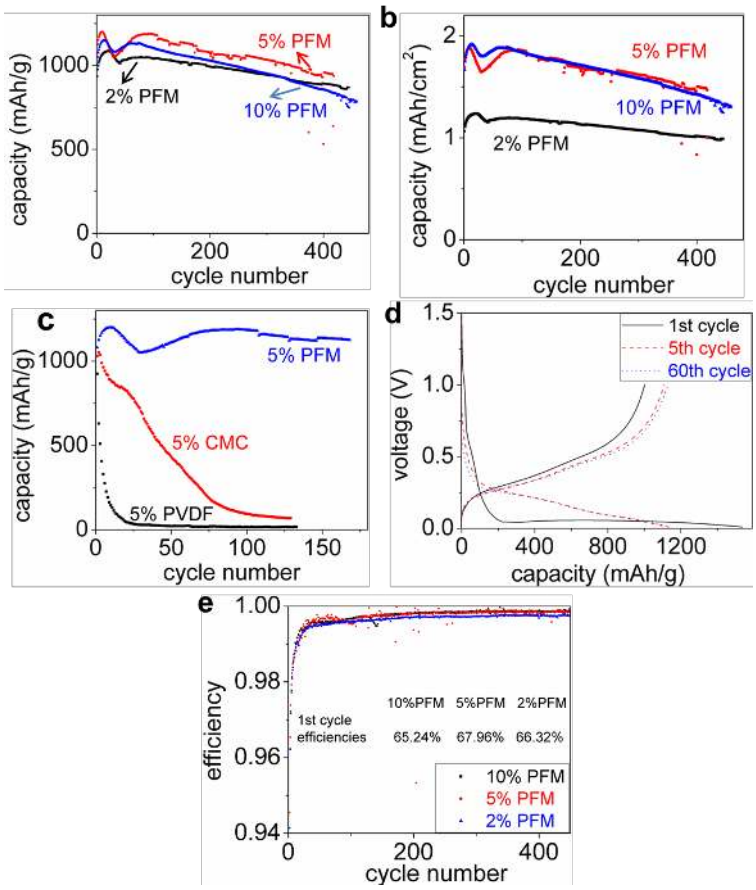

Figure 3. (a) Galvanostatic cycling performance of SiO anodes with 2%, 5%, and 10% by weight of a PFM binder using lithium counter electrodes at a C/10 rate (200 mA/g). (b) The same data from (a) plotted in areal loading. (c) Comparison of the electrochemical performance of SiO electrodes made with 5% by weight of PVDF, CMC, and PFM binders using lithium counter electrodes at a C/10 rate. (d) 1st, 5th, and 60th cycle potential vs. the capacity curves of a 2% PFM/SiO electrode. (e) Coulombic efficiencies of the three PFM-based cells.

SiO/PFM electrode performance. Figure 3 a and b show the galvanostatic cycling performance of SiO with a lithium metal counter electrode at a C/10 (200 mA/g) rate. For all three compositions, the cell capacities initially slightly increase to a peak capacity value, then decrease to maintain a stable cycling performance. The initial capacity fluctuation is due to the wetting of the PFM-based laminate. When using a similar functional conductive polymer binder with improved polarity for wetting, cell capacity is stable, and there is no initial capacity fluctuation.[19] The functional conductive polymer binder PFM enables SiO electrode to maintain a reversible capacity of 1,000 mAh/g for over 400 cycles with a 2% to 10% PFM binder. The minor capacity decay in all cases can be traced to the decay and dendrite formation at the lithium counter

electrode, as indicated by the formation of the mossy lithium on the surface of the lithium metal after the long-term cycling shown in Figure S4. Figure S4 also shows that the SiO electrode maintains the mechanical integrity with only 2% PFM after extended full capacity cycling. Figure 3b indicates the loading of the SiO electrodes. The PFM content at 2% can successfully enable long-term full capacity reversible cycling of the SiO anode with ~1 mAh/cm^2 areal loading. The higher the areal loading, more binder is needed to maintain stable capacity.[22] The SiO electrode with a 10% binder is able to maintain an areal capacity of 2 mAh/cm^2 for about 100 cycles. This also demonstrated the importance of adhesion in accommodating stress and maintaining electrode mechanical stability. Note that most of the previous work in the development of a silicon electrode for LIBs only has an areal capacity less than 1 mAh/cm^2.[4] SiO_x/SiO_y bilayer nano-membranes were recently developed as anodes, which reaches a capacity of ~1200 mAh/g at C/10 for 100 cycles.[14] A SiO-Sn_xCoyC_z anode showed a capacity of ~1000 mAh/g at C/10 for 100 cycles.[23] Helical silicon/silicon oxide core-shell structure was used as anode on to the surface of bulk silicon, although a high specific capacity was shown (~1700 mAh/g), but only lasted for ~70 cycles.[24] Note that the SiO anode enabled by conductive polymer binder exhibits long term cycling stability (over 500 cycles) with high capacity (900~1000 mAh/g), the loading (areal capacity of ~2 mAh/cm^2) is high compared to most literature reports, and this optimum performance only requires 5% conductive polymer and 95% active SiO materials without any conductive additives.

Compared to conventional binders, the advantage of the conductive PFM binder is further confirmed in Figure 3c. The PVDF binder has no electric conductivity, nor does it chemically bond with SiO, therefore fast fading occurs and the capacity drops to almost zero after 20 cycles.

The CMC binder has carboxylate functional groups that are known to form chemical bonding with the surface hydroxide group on Si-based materials, however, the CMC binder lacks electric conductivity.[25] The bonding with only 5% CMC binder in the laminate was not able to maintain good electrochemical performance. The SiO electrode only needs as little as 2% functional conductive PFM binder to outperform most other binders. The voltage curves of the fifth cycle and sixtieth cycles almost overlap, indicating minimum capacity decay during cycling. Figure S5 shows the TEM morphologies of pristine SiO electrodes with 2% PFM and after 30 cycles at C/10. The crystalline phase disappears after cycling, corresponding to the transition of the crystalline silicon to an amorphous phase, which is confirmed by the completely blurred electron diffraction image. The TEM image after 30 cycles (Figure S5b) also shows that the PFM polymer indeed maintains the mechanical integrity of electrodes throughout the battery operation. However, the TEM images of the surface of the particles before and after cycling are similar, without a thick layer of electrolyte-decomposed products on the cycled SiO particles.[26] The SEM electrode morphologies of the three PFM-based electrodes were also characterized and are shown in Figure S6. The polymer network is very important to maintain the structure of the electrode, which was also shown recently by other binder chemistry.[27] An apparent large porosity is also shown in the pristine electrode image, and electrolyte decomposition clearly occurs after one cycle. The SEM images show that the solid electrolyte interphase (SEI) products are not excessive. This controlled SEI formation plays an important role[28,29] for the long-term reversible cycling shown in Figure 3.

With 5% PFM, the CE of the cell is as high as 99.62% at the sixtieth cycle. High CE is critical for the long-term stable cycling of the anode electrode and better capacity retention at the full cell level. The first cycle CE is only ~65% (Table S1), which is comparable to its value in

most of the literature value. Besides the formation of SEI,[30] lithium reacts and converts silicon oxide to silicate, which contributes to the large first cycle irreversible capacity.[31] This is a detrimental problem in a lithium-ion cell, since the lithium ions from the cathode will be irreversibly consumed.[32] To compensate for the irreversible capacity loss in the first cycle, stabilized lithium metal powder (SLMP®) is used to prelithiate the SiO anode in the SiO/Lithium Nickel Manganese Cobalt Oxide ($LiNi_{1/3}Mn_{1/3}Co_{1/3}O_2$) (NMC) full cell. SLMP is a micro-size lithium metal powder with ~2 wt% lithium carbonate surface coating (Figure 4b).[33,34] SLMP prelithiation of a silicon-carbon nanotube anode was shown to improve the first cycle CE in a full cell from 52% to almost 100%.[35] A recent study from our group also showed that prelithiation of graphite effectively compensated for the first-cycle loss and formed a fully functional SEI on the graphite anode, in both a half cell and a graphite/NMC full cell.[36]

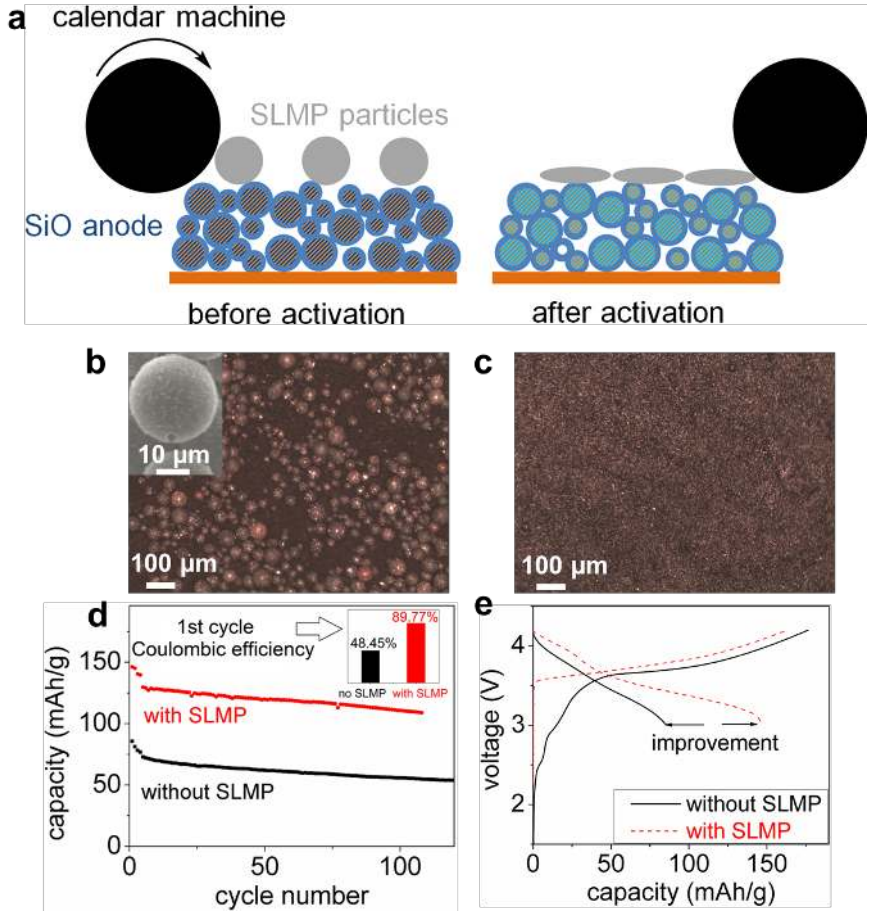

Figure 4. (a) Schematics of the utilization of SLMP for the SiO electrode. SLMP particles are loaded on to the SiO anode. Rolling compression was used to crush the Li_2CO_3 shell of SLMP to release lithium metal and laminate it on the surface of SiO electrode. This process is called SLMP activation. (b) SLMP particles loaded on the SiO electrode before activation. The inset shows the SEM image of a single SLMP particle. (c) The SiO electrode surface after electrolytes are added onto the SiO electrode with activated SLMP after 12 hours. This shows the disappearance of SLMP and indicates the successful prelithiation of the SiO electrode. (d) SiO/NMC full cell performance with or without the SLMP capacity-enhancement additive, two cycles at C/20, two cycles at C/10, and then C/3. (e) The first cycle voltage curves of the two cells.

Full cell performance improved by SLMP. SLMP was directly loaded on top of the dried SiO anode, which proved to be a simple and effective way of applying SLMP.[36] The amount of loaded SLMP was calculated to theoretically eliminate all the irreversible capacity in the first cycle. A calendar machine was used to pressure-activate the SLMP particles (Figure 4a). This operation breaks the lithium carbonate (Li_2CO_3) shell and allows lithium to be in direct electrical contact with the SiO materials in the anode.[37] The shape change of SLMP could be seen before (Figure 4b) and after (Figure S7d) pressure-activation of the SLMP. When it makes contact with the electrolyte, the SLMP on the SiO electrode releases lithium which spontaneously migrates to SiO. SEI formation is induced, and partial lithiation of the SiO also occurs, indicated by the disappearance of SLMP in Figure 4c. A 96-hour rest period was used to allow the crushed SLMP to fully prelithiate the SiO anode before current-driven charging of the cells. As a good control, the SiO/NMC full cell without SLMP was also rested for 96 hours before cycling. Both full cells were put in a formation process consisting of two cycles at C/20 and two cycles at C/10 prior to C/3 cycling. Apparent improvement was shown for the SLMP-loaded full cells. The first cycle CE increased from 48% to ~90% with the SLMP (shown in the inset of Figure 4d). SLMP enabled the NMC/SiO full cell to maintain a reversible capacity of ~110 mAh/g after more than 100 cycles at C/3.[38] Part of the lithium in the NMC cathode was irreversibly consumed by SiO without SLMP

prelithiation. The full cell without SLMP prelithiation started only with a capacity of ~80 mAh/g and dropped to ~50 mAh/g after 100 cycles.

The first cycle voltage curves of the full cells are shown in Figure 4e. Compared to the regular cell without SLMP, the voltage profile at both ends (start of charge and end of discharge) are distinctly different, indicating different lithiation and delithiation of SiO during these two stages. In the first cycle charge process, SLMP eliminated the needs for SEI formation and silica conversion, so the curve goes directly to the anode lithiation voltage region. When SLMP is not used, this charging curve shows a long multi-plateau curvature accounting for a capacity of ~40 mAh/g, which is typical for irreversible processes of SiO conversion and SEI formation. Not only is the cell capacity stable during cycling, the voltages between charge and discharge remain stable from the first cycle to the fortieth cycle (Figure S9b). The excellent electrochemical performance demonstrates the superb SiO surface and electrode mechanical stability. The SEM image of the SiO electrode rested for 96 hours in a full cell without SLMP is shown in Figure S9c. Compared to the pristine electrode (Figure S6), no apparent morphology change occurred during this equilibration period. When the SiO/NMC full cell is loaded with SLMP on the SiO electrode, the SEM image in Figure S9d shows a clear SEI formation due to the electrolyte decomposition after 96-hour rest period. The SEI formation and partial lithiation of the SiO particles could be further confirmed by the particle size analysis. The size of SiO particles after resting in SiO/NMC/SLMP cell (Figure S9f) shows a bigger value compared to the control sample without SLMP (Figure S9e).

Discussion

In a typical Si system, the surface Si element participates in the alloy reaction with the lithium elements. The potential bond breaking between the Si surface and binder weakens the adhesion over cycling, so a high concentration of binder is required.[39] However, in the SiO system, the nano-Si domains are distributed in the SiO_2 matrix. The surface is predominately SiO_2, and it does not participate in the alloy reaction; rather, it maintains the surface functional bonding during cycling. The existence of the enhancing SiO_2 domains on the surface allows the use of less binder but achieve similar binding strength. Because of the existence of the stable SiO_2 phase, the binder functions very effectively during cell operation. Also, a special electrode design is required to accommodate the large volume change of Si during cycling to build a higher-loading electrode.[5,6] SiO, with nano-active Si domains dispersed in the silica as a buffer phase, not only has improved dimensional stability and reduced side reactions, but also improves adhesion in combination with the functional conductive polymer binder. The ester bond between the adhesion functional group of the PFM and SiO_2 matrix surface (Figure 2c) is maintained throughout the lithiation and delithiation process. Therefore, A high-concentration and areal-loading SiO (~1000 mAh/g) electrode can be achieved, as shown in Figure 3.[40] The SiO electrodes with 2% to 10% PFM functional conductive polymer binder have at least three times more practical energy density than that of a state-of-the-art graphite electrode.

The calculated energy densities of the NMC/SiO full cell (Figure S10) indicate that the application of SLMP to prelithiate SiO enables 20%~30% improvement compared to the graphite/NMC full cell. However, without SLMP prelithiation, the SiO/NMC full cell only delivers ~70% of the capacity of the state-of-the-art graphite/NMC due to the consumption of lithium during SiO activation. SiO has attracted more and more attention recently as promising

anode candidate for LIBs, however, high active material content and the compensation for the first cycle irreversible capacity, are critical to achieve the full potential of this material.

In conclusion, SiO electrodes were cycled in stable and high gravimetric capacity (>1000 mAh/g) using a functional conductive polymer binder in composite electrodes. Compared to other conventional binders such as PVDF and CMC, the conductive functional polymer binder used in the SiO system shows obvious advantages because of its electrical conductivity and strong adhesion. The loading of SiO in the electrode can be as high as 98 wt%, and the half cell with this laminate shows a capacity higher than 1000 mAh/g up to ~ 500 cycles. The use of SLMP improves the first cycle CE from ~48% to ~90%, and greatly enhances the energy density of the SiO/NMC full cell. The combined strategy of using both a functional conductive polymer binder and an SLMP prelithiation solves the volume expansion and low first-cycle coulombic efficiency problems, leading to a high-energy lithium-ion chemistry.

References

1. Boukamp, B. A.; Lesh, G. C.; Huggins, R. A. *Journal of The Electrochemical Society* **1981,** 128, (4), 725-729.
2. Li, J.; Dahn, J. R. *Journal of The Electrochemical Society* **2007,** 154, (3), A156-A161.
3. Ryu, J. H.; Kim, J. W.; Sung, Y.-E.; Oh, S. M. *Electrochemical and Solid-State Letters* **2004,** 7, (10), A306-A309.
4. Kovalenko, I.; Zdyrko, B.; Magasinski, A.; Hertzberg, B.; Milicev, Z.; Burtovyy, R.; Luzinov, I.; Yushin, G. *Science* **2011,** 334, (6052), 75-79.
5. Xun, S.; Xiang, B.; Minor, A.; Battaglia, V.; Liu, G. *Journal of The Electrochemical Society* **2013,** 160, (9), A1380-A1383.
6. Liu, N.; Lu, Z.; Zhao, J.; McDowell, M. T.; Lee, H.-W.; Zhao, W.; Cui, Y. *Nature Nanotechnology* **2014,** 9, 187-192.
7. AlKaabi, K.; Prasad, D. L. V. K.; Kroll, P.; Ashcroft, N. W.; Hoffmann, R. *Journal of the American Chemical Society* **2014,** 136, (9), 3410-3423.
8. Kim, T.; Park, S.; Oh, S. M. *Journal of The Electrochemical Society* **2007,** 154, (12), A1112-A1117.
9. Nagao, Y.; Sakaguchi, H.; Honda, H.; Fukunaga, T.; Esaka, T. *Journal of The Electrochemical*

Society **2004,** 151, (10), A1572-A1575.

10. Su, X.; Wu, Q.; Li, J.; Xiao, X.; Lott, A.; Lu, W.; Sheldon, B. W.; Wu, J. *Advanced Energy Materials* **2014,** 4, 1300882.

11. Miyachi, M.; Yamamoto, H.; Kawai, H. *Journal of The Electrochemical Society* **2007,** 154, (4), A376-A380.

12. Kim, J.-H.; Sohn, H.-J.; Kim, H.; Jeong, G.; Choi, W. *Journal of Power Sources* **2007,** 170, (2), 456-459.

13. Jing, S.-Y.; Lee, H.-J.; Choi, C. K. *Journal of the Korean Physical Society* **2002,** 41, (5), 769-773.

14. Zhang, L.; Deng, J.; Liu, L.; Si, W.; Oswald, S.; Xi, L.; Kundu, M.; Ma, G.; Gemming, T.; Baunack, S.; Ding, F.; Yan, C.; Schmidt, O. G. *Advanced Materials* **2014,** 26, (26), 4527-4532.

15. Yuca, N.; Zhao, H.; Song, X.; Dogdu, M. F.; Yuan, W.; Fu, Y.; Battaglia, V. S.; Xiao, X.; Liu, G. *ACS Applied Materials & Interfaces* **2014**.

16. Zhao, H.; Zhou, X.; Park, S.-J.; Shi, F.; Fu, Y.; Ling, M.; Yuca, N.; Battaglia, V.; Liu, G. *Journal of Power Sources* **2014,** 263, (0), 288-295.

17. Ling, M.; Qiu, J.; Li, S.; Zhao, H.; Liu, G.; Zhang, S. *Journal of Materials Chemistry A* **2013,** 1, (38), 11543-11547.

18. Liu, G.; Xun, S.; Vukmirovic, N.; Song, X.; Olalde-Velasco, P.; Zheng, H.; Battaglia, V. S.; Wang, L.; Yang, W. *Advanced Materials* **2011,** 23, (40), 4679-4683.

19. Wu, M.; Xiao, X.; Vukmirovic, N.; Xun, S.; Das, P. K.; Song, X.; Olalde-Velasco, P.; Wang, D.; Weber, A. Z.; Wang, L. W.; Battaglia, V. S.; Yang, W.; Liu, G. *J Am Chem Soc* **2013,** 135, (32), 12048-56.

20. Dai, K.; Zhao, H.; Wang, Z.; Song, X.; Battaglia, V.; Liu, G. *Journal of Power Sources* **2014,** 263, (0), 276-279.

21. Stournara, M. E.; Xiao, X.; Qi, Y.; Johari, P.; Lu, P.; Sheldon, B. W.; Gao, H.; Shenoy, V. B. *Nano Letters* **2013,** 13, (10), 4759-4768.

22. Chen, J.; Liu, J.; Qi, Y.; Sun, T.; Li, X. *Journal of The Electrochemical Society* **2013,** 160, (9), A1502-A1509.

23. Liu, B.; Abouimrane, A.; Ren, Y.; Balasubramanian, M.; Wang, D.; Fang, Z. Z.; Amine, K. *Chemistry of Materials* **2012,** 24, (24), 4653-4661.

24. Yoo, H.; Lee, J.-I.; Kim, H.; Lee, J.-P.; Cho, J.; Park, S. *Nano Letters* **2011,** 11, (10), 4324-4328.

25. Bridel, J. S.; Azaïs, T.; Morcrette, M.; Tarascon, J. M.; Larcher, D. *Chemistry of Materials* **2009,** 22, (3), 1229-1241.

26. Etacheri, V.; Haik, O.; Goffer, Y.; Roberts, G. A.; Stefan, I. C.; Fasching, R.; Aurbach, D. *Langmuir* **2011,** 28, (1), 965-976.

27. Song, J.; Zhou, M.; Yi, R.; Xu, T.; Gordin, M. L.; Tang, D.; Yu, Z.; Regula, M.; Wang, D. *Advanced Functional Materials* **2014,** 24, (37), 5904-5910.

28. Xu, K. *Chemical Reviews* **2004,** 104, (10), 4303-4418.

29. Shi, F.; Zhao, H.; Liu, G.; Ross, P. N.; Somorjai, G. A.; Komvopoulos, K. *The Journal of Physical Chemistry C* **2014,** 118, (27), 14732-14738.

30. Zhao, H.; Park, S.-J.; Shi, F.; Fu, Y.; Battaglia, V.; Ross, P. N.; Liu, G. *Journal of The Electrochemical Society* **2014,** 161, (1), A194-A200.

31. Chang, W.-S.; Park, C.-M.; Kim, J.-H.; Kim, Y.-U.; Jeong, G.; Sohn, H.-J. *Energy & Environmental Science* **2012,** 5, (5), 6895-6899.

32. Jeong, G.; Kim, Y.-U.; Krachkovskiy, S. A.; Lee, C. K. *Chemistry of Materials* **2010,** 22, (19), 5570-5579.

33. Jarvis, C. R.; Lain, M. J.; Gao, Y.; Yakovleva, M. *Journal of Power Sources* **2005,** 146, (1–2), 331-334.
34. Jarvis, C. R.; Lain, M. J.; Yakovleva, M. V.; Gao, Y. *Journal of Power Sources* **2006,** 162, (2), 800-802.
35. Forney, M. W.; Ganter, M. J.; Staub, J. W.; Ridgley, R. D.; Landi, B. J. *Nano Letters* **2013,** 13, (9), 4158-4163.
36. Wang, Z.; Fu, Y.; Zhang, Z.; Yuan, S.; Amine, K.; Battaglia, V.; Liu, G. *Journal of Power Sources* **2014,** 260, 57-61.
37. Xiang, B.; Wang, L.; Liu, G.; Minor, A. M. *Journal of The Electrochemical Society* **2013,** 160, (3), A415-A419.
38. Cai, L.; Dai, Y.; Nicholson, M.; White, R. E.; Jagannathan, K.; Bhatia, G. *Journal of Power Sources* **2013,** 221, (0), 191-200.
39. Beattie, S. D.; Larcher, D.; Morcrette, M.; Simon, B.; Tarascon, J.-M. *Journal of The Electrochemical Society* **2008,** 155, (2), A158-A163.
40. Wu, H.; Cui, Y. *Nano Today* **2012,** 7, (5), 414-429.

ASSOCIATED CONTENT

Supplementary Information

Details about materials synthesis and characterizations, battery assembly and testing, electrochemical measurements, comparison of the energy densities with or without SLMP. This material is available free of charge via the Internet at http://pubs.acs.org

AUTHOR INFORMATION

Corresponding Author

*E-mail: gliu@lbl.gov

Notes

The authors declare no competing financial interests.

ACKNOWLEDGEMENTS

This work was funded by the Assistant Secretary for Energy Efficiency, Office of Vehicle Technologies of the U.S. Department of Energy (U.S. DOE) under contract no. DE-AC02-05CH 11231 under the Batteries for Advanced Transportation Technologies (BATT) Program. The

authors acknowledge support of the National Center for Electron Microscopy, Lawrence Berkeley Lab, which is supported by the U.S. Department of Energy under Contract # DE-AC02-05 CH11231. G.L. thanks Robert R. Powell at General Motors for the helpful discussion and guidance.

TOC